SCIENCE CHINA
Information Sciences

• LETTER •

July 2024, Vol. 67, Iss. 7, 179302:1–179302:2
https://doi.org/10.1007/s11432-023-4024-2

Channel modeling for MI-based wireless underground sensor networks with conductive objects

Shuhan DENG[1], Guanghua LIU[1*], Ziwei CHEN[1,2], Huaijin ZHANG[1,2] & Tao JIANG[1]

[1]*Research Center of 6G Mobile Communications, School of Cyber Science and Engineering, Huazhong University of Science and Technology, Wuhan* 430074*, China;*
[2]*School of Electronic Information and Communications, Huazhong University of Science and Technology, Wuhan* 430074*, China*

Received 12 August 2023/Revised 12 March 2024/Accepted 6 May 2024/Published online 27 June 2024

Wireless underground sensor networks (WUSNs) are an emerging research field with promising applications. However, WUSNs links suffer from significant attenuation as the propagation of the signal needs to pass through soil, rock, and water. Magnetic induction (MI)-based transmission is proposed to overcome these issues as MI signal can penetrate most substances similarly without experiencing high path loss, which ensures the robustness of WUSNs links [1]. However, the actual underground environment often contains conductive objects that can generate eddy currents and secondary magnetic fields. The traditional channel models are no longer suitable. As a result, developing an accurate channel model with conductive objects is crucial, which is the foundation for designing the MI-WUSNs system.

To this end, related contributions have been made to characterize the MI channel with conductive objects. Some studies utilize numerical models through electromagnetic simulations to investigate the effect of metals on the MI system. However, the numerical models are unable to characterize the relationships between various parameters. An analytical channel model is still indispensable. Ref. [2] developed an analytical solution of the induced voltage in receiving coils through an infinite metal plate. Ref. [3] proposed a semi-analytic model to quantify the effects of a metallic corona ring on magnetic coupling. The MI channel model in thick conductive pipes considering the attenuation effect of metals is further developed in [4]. Nevertheless, there is still a gap in accurate channel modeling with metal plates of finite size, which is more realistic for underground environments. In this study, we develop an analytical channel model for MI-based WUSNs and carry out the experimental validation.

Channel modeling. The MI channel with conductive objects can be equated to three types of circuits: transmitter circuit, receiver circuit, and metallic circuit, which are coupled to each other, as shown in Figure 1. One conductive object is equated to one metallic circuit consisting of an inductance L_m and a resistance R_m. U_s is the voltage of the signal source; R_s is its resistance; L_t and L_r are the equivalent inductances of the transmitter and receiver coils; C_t and C_r are the capacitances of the coils; R_t and R_r are the resistances of the coils; R_L is the load impedance of the receiver circuit. The whole derivation of circuit parameters is given in Appendix A. The impedances of the transmitter, receiver and metallic circuits are $Z_t = R_t+R_s+\mathrm{j}\omega L_t+\frac{1}{\mathrm{j}\omega C_t}$, $Z_r = R_r + \mathrm{j}\omega L_r + \frac{1}{\mathrm{j}\omega C_r} + R_L$, $Z_m = R_m + \mathrm{j}\omega L_m$, respectively, where ω is the angular frequency of MI signal.

When a conductive object is present in a varying magnetic field, eddy currents are generated and excite a secondary magnetic field. We then divide the secondary induction by the secondary magnetic field into two cases: reflection and refraction. Reflection occurs when the conductor is positioned parallel to the coil axis, while refraction occurs when the conductor is placed vertically. Assuming there are p reflection conductors and q refraction conductors, as shown in Figure 1. The reflection and refraction conductors are recorded as $1, 2, \ldots, p$ and $p+1, p+2, \ldots, p+q$. The positions and sizes of all objects are known by conductor detection.

By considering the ith reflection conductors with length W, height H and thickness l, the mutual inductances of the coils and the conductor can be derived respectively [5]

$$M_{t,i} \approx \frac{\mu\pi N_t a_t^2 W^2 H^2}{4d_{tm}^3}\left|\cos\theta_t \cdot \cos\theta_{tm} - \frac{1}{2}\sin\theta_t \cdot \sin\theta_{tm}\right|, \tag{1}$$

$$M_{r,i} \approx \frac{\mu\pi N_r a_r^2 W^2 H^2}{4d_{rm}^3}\left|\cos\theta_r \cdot \cos\theta_{rm} - \frac{1}{2}\sin\theta_r \cdot \sin\theta_{rm}\right|, \tag{2}$$

where μ is the permittivity of the soil; N_t and N_r are the number of turns of the transmitter and receiver coils; a_t and a_r are the radius of the coils; d_{tm} is the distance between the object and the transmitter coil; d_{rm} is the distance between the object and the receiver coil; θ_t, θ_r, θ_{tm}, θ_{rm} are the angles between the coils and the object.

Considering the ith refraction conductor with length W, height H and thickness l, the primary magnetic field generated by the coil is shielded by the conductor. We introduce the loss factor $S = \mathrm{e}^{-l\sqrt{\frac{\omega\mu_m\sigma}{2}}}$ to represent the attenuation, where μ_m and σ are the permeability and conductivity of the conductor. The thicker the conductor, the greater the attenuation. Additionally, due to the limited size of the object, only a portion of the magnetic field is shielded,

* Corresponding author (email: guanghualiu@hust.edu.cn)

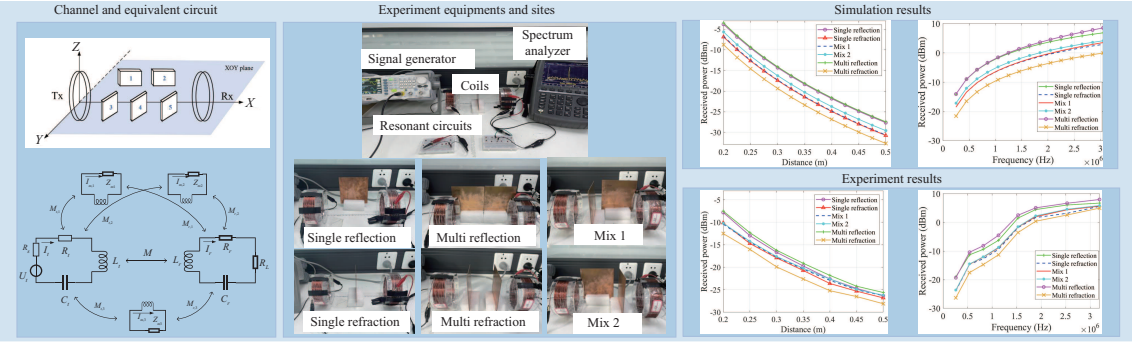

Figure 1 (Color online) MI channel and experimental results.

while the rest propagates around the object. Therefore, the shielding factor α is introduced, calculated by the ratio of the magnetic flux passing through the surface of the object to the total magnetic flux in the plane of the surface, $\alpha = \int_{\frac{-H}{2}}^{\frac{H}{2}} \int_{\frac{-W}{2}}^{\frac{W}{2}} \frac{(2x_0{}^2-y^2-z^2)}{4\pi\left(x_0^2+y^2+z^2\right)^{2.5}} \mathrm{d}y\mathrm{d}z \Big/ \int_0^{\alpha_0} \frac{b(2x_0^2-b^2)}{2\left(b^2+x_0{}^2\right)^{2.5}} \mathrm{d}b$, where x_0 is the distance of the conductive object from the coil on the x-axis, α_0 is the approximate range of the magnetic field. The detailed derivation of the shielding factor is given in Appendix B. The shielding factor of q refractive conductive objects are $\alpha_1, \alpha_2, \ldots, \alpha_q$, respectively.

The original mutual induction of the transmitter and receiver coils is $M \simeq \mu\pi N_t N_r \frac{a_t^2 a_r^2}{2d^3}$. After being affected by conductive objects (only refraction conductors), it becomes

$$M' = M(\alpha_1 S+1-\alpha_1)(\alpha_2 S+1-\alpha_2)\cdots(\alpha_q S+1-\alpha_q). \quad (3)$$

The mutual inductance between the ith reflection conductor and the coils can be derived respectively

$$M'_{t,i} = M_{t,i}(\alpha_1 S+1-\alpha_1)(\alpha_2 S+1-\alpha_2)\cdots(\alpha_{i-1} S+1-\alpha_{i-1}), \quad (4)$$

$$M'_{r,i} = M_{r,i}(\alpha_{i+1} S+1-\alpha_{i+1})(\alpha_{i+2} S+1-\alpha_{i+2}) \cdots(\alpha_q S+1-\alpha_q). \quad (5)$$

The circuit equations are given by Kirchhoff's voltage law

$$\begin{cases} Z_t I_t - \sum_{i=1}^{p} \mathrm{j}wM_{t,i}I_{m,i} - \sum_{i=p+1}^{p+q} \mathrm{j}wM'_{t,i}I_{m,i} - \mathrm{j}wM'I_r = U_s, \\ Z_r I_r - \sum_{i=1}^{p} \mathrm{j}wM_{r,i}I_{m,i} - \sum_{i=p+1}^{p+q} \mathrm{j}wM'_{r,i}I_{m,i} - \mathrm{j}wM'I_t = 0, \\ Z_{m,1}I_{m,1} - \mathrm{j}wM_{t,1}I_t - \mathrm{j}wM_{r,1}I_r = 0, \\ \vdots \\ Z_{m,p}I_{m,p} - \mathrm{j}wM_{t,p}I_t - \mathrm{j}wM_{r,p}I_r = 0, \\ Z_{m,(p+1)}I_{m,(p+1)} - \mathrm{j}wM'_{t,(p+1)}I_t - \mathrm{j}wM'_{r,(p+1)}I_r = 0, \\ \vdots \\ Z_{m,(p+q)}I_{m,(p+q)} - \mathrm{j}wM'_{t,(p+q)}I_t - \mathrm{j}wM_{r,(p+q)}I_r = 0, \end{cases} \quad (6)$$

where $Z_{m,1}, \ldots, Z_{m,p}$ and $Z_{m,p+1}, \ldots, Z_{m,p+q}$ are the impedances of reflection and refraction conductors. $I_{m,i}$, I_t and I_r denote the current in the ith object, transmitter coil and receiver coil. By solving the equations, we derive the received current and received power

$$I_r = \frac{\sum_{i=1}^{p} \mathrm{j}wM_{r,i}I_{m,i} - \sum_{i=p+1}^{p+q} \mathrm{j}wM'_{r,i}I_{m,i} + \mathrm{j}wM'I_t}{Z_r}, \quad (7)$$

$$P_r = \frac{1}{2}|I_r|^2 R_L. \quad (8)$$

Numerical and experimental analysis. We discuss the numerical and experimental results of the MI channel with conductive objects in order to validate the accuracy of our channel model and investigate the impact of conductive objects on the MI system. Our experimental scenario and results are shown in Figure 1. We explore various scenarios involving single and multiple conductive objects. The experimental variation tendency is in accordance with the simulation. The results show that reflection conductors lead to an improvement in received power, while refraction conductors cause attenuation. Additionally, both the number and the position of the objects have effects on received power. The setup and analysis of our experiment are given in Appendix C.

Conclusion. We develop a comprehensive and accurate channel model for MI-WUSNs by taking into account the impact of multiple conductive objects located in different positions. The mathematical expressions for mutual inductance and received power are rigorously derived for each case. Extensive experimental results have verified our theory. Hence, this paper provides a solid foundation for subsequent system design for MI-WUSNs.

Acknowledgements This work was supported by National Natural Science Foundation of China (Grant No. 62371200) and Young Elite Scientists Sponsorship Program by CAST (Grant No. 2023QNRC001).

Supporting information Appendixes A–C. The supporting information is available online at info.scichina.com and link.springer.com. The supporting materials are published as submitted, without typesetting or editing. The responsibility for scientific accuracy and content remains entirely with the authors.

References

1 Liu G. Data collection in MI-assisted wireless powered underground sensor networks: directions, recent advances, and challenges. IEEE Commun Mag, 2021, 59: 132–138
2 Xiao C, Wei K, Cheng D, et al. Wireless charging system considering eddy current in cardiac pacemaker shell: theoretical modeling, experiments, and safety simulations. IEEE Trans Ind Electron, 2017, 64: 3978–3988
3 Liang H W R, Wang H, Lee C K, et al. Analysis and performance enhancement of wireless power transfer systems with intended metallic objects. IEEE Trans Power Electron, 2020, 36: 1388–1398
4 Guo H, Prince M, Ramsey J J S, et al. A low-cost through-metal communication system for sensors in metallic pipes. IEEE Sens J, 2023, 23: 8952–8960
5 Tan X, Sun Z. Environment-aware indoor localization using magnetic induction. In: Proceedings of IEEE Global Communications Conference, 2015. 1–6